Molecular Pharmacology Fast Forward. Published on January 8, 2019 as DOI: 10.1124/mol.118.114405
This article has not been copyedited and formatted. The final version may differ from this version.

MOL # 114405

Title Page

Inhibition of interleukin 10 transcription through the SMAD2/3 signaling pathway by Ca^{2+}-activated K^+ channel $K_{Ca}3.1$ activation in human T-cell lymphoma HuT-78 cells

Miki Matsui[1,2], Junko Kajikuri[2], Hiroaki Kito[2], Kyoko Endo[1,2], Yuki Hasegawa[1], Shinya Murate[2], Susumu Ohya[2]

[1]Department of Pharmacology, Kyoto Pharmaceutical University, Kyoto 607-8414, Japan

[2]Department of Pharmacology, Graduate School of Medical Sciences, Nagoya City University, Nagoya 467-8601, Japan

Molecular Pharmacology Fast Forward. Published on January 8, 2019 as DOI: 10.1124/mol.118.114405
This article has not been copyedited and formatted. The final version may differ from this version.

MOL # 114405

Running title page

Running title: K_{Ca}3.1 activation-induced IL-10 down-regulation

Corresponding author: Susumu Ohya, Ph.D., Department of Pharmacology, Graduate School of Medical Sciences, Nagoya City University, Nagoya 467-8601, Japan; Tel.: +81-52-853-8149; E-mail: sohya@med.nagoya-cu.ac.jp

Number of text pages: 33

Number of tables: 0

Number of figures: 8

Number of references: 47

Number of words in the *Abstract*: 247

Number of words in the *Introduction*: 650

Number of words in the *Discussion*: 1040

Abbreviations: ACTB, β-actin; AM, acetoxymethyl ester; Blimp, B-lymphocyte-induced maturation protein; CD, cluster of differentiation; CRAC, Ca^{2+} release-activated Ca^{2+} channel; CaMK, Ca^{2+}/calmodulin-dependent protein kinase; DCEBIO, 5,6-dichloro-1-ethyl-1,3-dihydro-2H-benzimidazol-2-one; DMSO, dimethyl sulfoxide; EGR, early growth response gene; ELISA; enzyme-linked immunosorbent assay (ELISA), E4BP, E4 promoter–binding protein; Foxp, forkhead box P; HDAC, histone deacetylase; Ig, immunoglobulin; IL, interleukin; K_{Ca}, Ca^{2+}-activated K^+ (channel); LAG; lymphocyte-activation gene; MAPK, mitogen-activated protein kinase; MTMR6, phosphatidylinositol 3-phosphate myotubularin-related protein; mTOR, mammalian target of rapamycin; NDPK, nucleoside diphosphate

kinase; NFAT, nuclear factor of activated T cells; NF-κB, nuclear factor-kappa B; NIH, National Institute of Health; PCR, polymerase chain reaction; PGAM, phosphoglycerate mutase family member; PHPT, protein histidine phosphatase; PI3K-C2, class II phosphoinositide 3-kinase; STAT, signal transducers and activator of transcription; TGF, transforming growth factor; Th, helper T (cell); Treg, regulatory T (cells); TRIM, tripartite motif (family); TRP, transient receptor potential.

Molecular Pharmacology Fast Forward. Published on January 8, 2019 as DOI: 10.1124/mol.118.114405
This article has not been copyedited and formatted. The final version may differ from this version.

Abstract

The hyperpolarization induced by intermediate-conductance Ca^{2+}-activated K^+ channel ($K_{Ca}3.1$) activation increases the driving force for Ca^{2+} influx, which generally promotes cell proliferation, migration, and cytokine production in immunocompetent cells. Interleukin-10 (IL-10) from tumor-infiltrating lymphocytes and macrophages, lymphoma, and carcinoma cells facilitates escape from cancer immune surveillance; however, the role of $K_{Ca}3.1$ in IL-10 production remains unclear. The objective of the present study is to elucidate the involvement of $K_{Ca}3.1$ in IL-10 expression and production using the human T-cell lymphoma HuT-78 cells. In HuT-78 cells, IL-10 gene expression and production were reduced by the treatment with the $K_{Ca}3.1$ activator for 6 hr. Western blotting showed that the protein expression ratio of phospho-Smad2 (P-Smad2)/Smad2, but not P-Smad3/Smad3 was decreased by the treatment with $K_{Ca}3.1$ activator in HuT-78 cells. Concomitant with this, the nuclear translocation of P-Smad2 was inhibited by $K_{Ca}3.1$ activator. Furthermore, the $K_{Ca}3.1$ activator-induced transcriptional repression of IL-10 disappeared with the pre-treatment with the calmodulin kinase II (CaMKII) inhibitor, KN-62 for 1 hr, and $K_{Ca}3.1$ activator-induced decreases in the nuclear translocation of P-Smad2 were also prevented by the pre-treatment with KN-62. Taken together, the $K_{Ca}3.1$ activator-induced transcriptional repression of IL-10 is due to the inhibition of the nuclear translocation of P-Smad2 in HuT-78 cells, resulting in the prevention of P-Smad2/3 complex formation in nuclei, and the activation of CaMKII induced by $K_{Ca}3.1$ activators suppresses the constitutive activation of P-Smad2/3 in HuT-78 cells. Therefore, $K_{Ca}3.1$ activators have potential as a therapeutic option to suppress the tumor-promoting activities of IL-10.

Introduction

The anti-inflammatory cytokine, interleukin-10 (IL-10) is an immunosuppressive factor involved in tumorigenesis, and plays a crucial role in escape from cancer immune surveillance (Hamidullah et al., 2012). IL-10 expression is associated with lymphoproliferative disorders, such as lymphocytic leukemia, lymphoma, and myeloma (Benjamin et al., 1992; Finke et al., 1993; Lu et al., 1995). Increased IL-10 levels in patients with lymphoma are associated with poor survival due to the facilitation of tumor immune escape (Blay et al., 1993). IL-10 is frequently up-regulated in various types of cancers (Sato et al., 2011), and the inhibition of IL-10 accelerates apoptosis in breast cancer cells (Alotaibi et al., 2018). The T-cell lymphoma cell line HuT-78, which is Foxp3/CD25-negative and constitutively produces IL-10, has been used to study the underlying mechanisms of IL-10 expression in T cells (Mori et al., 1997; Tiffon et al., 2011). Mori et al. (1997) showed the involvement of the constitutive activation of NF-κB in the high level expression of IL-10 in HuT-78 cells. IL-10-producing naturally occurring regulatory T (T_{reg}) cells are Foxp3-positive $CD4^+CD25^+$ T cells and control autoimmunity (Itoh et al., 1999); however, recent studies showed that tumor-infiltrating Foxp3-negative $CD4^+$ $CD25^-$ T cells are naturally present as IL-10-secreting T cells (Burugu et al., 2017; Ma et al., 2017).

Ca^{2+}-activated K^+ (K_{Ca}) channels are classified into three subfamilies based on their unitary conductance: $K_{Ca}1.1$, $K_{Ca}2.x$ (2.1-2.3), and $K_{Ca}3.1$. In lymphoid and myeloid cells, membrane hyperpolarization by K^+ channel opening (i.e. $K_{Ca}3.1$, voltage-gated $K_V1.3$, and two-pore domain $K_{2P}5.1$) increased the activity of Ca^{2+} release-activated Ca^{2+} (CRAC) channels and transient receptor potential (TRP) Ca^{2+} channels (Cahalan & Chandy, 2009; Feske et al. ,2015; Ohya & Kito, 2018). The Ca^{2+}-dependent regulation of the transcription factors, NFAT, NF-κB, CaMKII, and MAPK, is involved in the activation of immune responses in T cells. $K_{Ca}3.1$

plays a pivotal role in the proliferation, differentiation, and migration of immune cells, and is a potential therapeutic target for autoimmune and inflammatory disorders. In addition, the enhancement of $K_{Ca}3.1$ activity promotes pro-inflammatory cytokine production and secretion by regulating Ca^{2+} signaling in $CD4^+$ T cells (Di et al., 2010; Ohya et al., 2014). In $CD8^+$ T cells with the capacity to kill malignant cells, K^+ efflux mediating $K_{Ca}3.1$ activation increases anti-tumor function by promoting IFN-γ production (Eil et al., 2016). The following positive and negative $K_{Ca}3.1$ function-modifying molecules have been identified in T cells: PI3K-C2B, NDPK-B, PHPT-1, MTMR6, PGAM-5, and TRIM-27 (Ohya & Kito, 2018). In T cells, $K_{Ca}3.1$ accumulates in the uropod, but not the leading edge, and is associated with oscillations in intracellular Ca^{2+} levels (Kuras et al., 2012). The pathological significance of $K_{Ca}3.1$ in IL-10-producing T cells and cancerous cells remains to be elucidated.

Smad2 and Smad3 (Smad2/3) are essential transcription factors in the development and maintenance of T_{reg} cells (Sekiya et al., 2016). Phosphorylated Smad2/3 (P-Smad2/3) translocate to the nucleus, together with Smad4, and activate the transcription of downstream target genes (Derynck & Zhang, 2003). The constitutive activation of Smad2/3 signaling is evoked by constitutive transforming growth factor (TGF)-β signaling in resting human $CD4^+$ T cells (Classen et al., 2007), and is maintained even in the presence of a TGF-β antagonist. Ca^{2+}/calmodulin-dependent protein kinase II (CaMKII) directly controls Smad2/3 function (Zimmerman et al., 1998; Wicks et al., 2000). The nuclear translocation of Smad2 is negatively regulated by Ca^{2+}-dependent CaMKII signaling, which disrupts the P-Smad2/3 complex formation (Ming et al., 2010). Limited information is currently available on the role of Smad2/3 in pro-inflammatory and anti-inflammatory cytokine expression.

We herein examined the effects of $K_{Ca}3.1$ activators on the transcriptional repression of IL-10 in HuT-78 cells. Our results indicated that IL-10 is a downstream target gene of the Smad2/3 signaling pathway, and $K_{Ca}3.1$ activators inhibit the nuclear translocation of P-Smad2,

Molecular Pharmacology Fast Forward. Published on January 8, 2019 as DOI: 10.1124/mol.118.114405
This article has not been copyedited and formatted. The final version may differ from this version.

which is constitutively active in HuT-78 cells. Our results also provide evidence for the importance of CaMKII signaling in the negative regulation of the nuclear translocation of Smad2 in HuT-78 cells.

Molecular Pharmacology Fast Forward. Published on January 8, 2019 as DOI: 10.1124/mol.118.114405
This article has not been copyedited and formatted. The final version may differ from this version.

Materials and Methods

Cell culture

The human T-cell lymphoma cell line HuT-78 was supplied by the RIKEN BioResource Center (RIKEN BRC) (Tsukuba, Japan). The human leukemic T-cell lymphoblast cell line, Jurkat clone E6, the human B lymphoma cell line, Daudi, the human chronic myeloid leukemia cell line, K562, and the human acute monocytic leukemia cell line, THP-1 were supplied by the Japanese Collection of Research Bioresources (JCRB) Cell Bank (Osaka, Japan) and Cell Resource Center for Biomedical Research (Sendai, Japan). Cells were maintained at 37°C, in 5% CO_2 with RPMI 1640 medium (Wako Pure Chemical Industries, Osaka, Japan) containing 10% fetal bovine serum (Sigma, St. Louis, MO, USA) and a penicillin-streptomycin mixture (Wako Pure Chemical Industries).

Real-time PCR assay

Total RNA extraction and reverse transcription from HuT-78, Jurkat, Daudi, K562, and THP-1 cells were performed as previously reported (Endo et al., 2015). cDNA products were amplified with gene-specific PCR primers, designated using Primer Express™ software (Ver 3.0.1, Thermo Fisher Scientific, Waltham, MA, USA). Quantitative real-time PCR was performed using SYBR Green chemistry on an ABI 7500 Fast real-time PCR system (Thermo Fisher Scientific). The following gene-specific PCR primers of human origin were used for real-time PCR: K_{Ca}1.1 (GenBank accession number, NM_001014797, 1120-1239), amplicon=120 bp; K_{Ca}2.1 (NM_002248, 649-764), 116 bp; K_{Ca}2.2 (NM_021614, 1492-1612), 121 bp; K_{Ca}2.3 (NM_002249, 2042-2146), 105 bp; K_{Ca}3.1 (NM_002250, 1475-1595), 121 bp; NDPK-B (NM_002512, 288-408), 121 bp; PI3K-C2B (NM_002646, 4052-4172), 121 bp; PHPT1 (NM_001135861, 783-903), 121 bp; MTMR6 (NM_004685, 1476-1607), 132 bp;

Molecular Pharmacology Fast Forward. Published on January 8, 2019 as DOI: 10.1124/mol.118.114405
This article has not been copyedited and formatted. The final version may differ from this version.

PGAM5 (NM_001170543, 277-396), 120 bp; TRIM-27 (NM_006510, 1580-1702), 123 bp; interferon (IFN)-γ (NM_000619, 403-522), 120 bp; interleukin (IL)-17A (NM_002190, 355-474), 120 bp; IL-4 (NM_000589, 287-406), 120 bp; IL-5 (NM_000879, 327-446), 120 bp; IL-13 (NM_002188, 166-285), 120 bp; IL-10 (NM_000572, 339-458), 120 bp; IL-32 (NM_001012631, 408-527), 120 bp; E4BP4 (NM_001289999, 1217-1339), 123 bp; GATA3 (NM_001002295, 1335-1454), 120 bp; cMAF (NM_005360, 1697-1818), 120 bp; Blimp1 (NM_001198, 1425-1544), 120 bp; CD25 (NM_000417, 750-869), 120 bp; Foxp3 (NM_014009, 1253-1372), 120 bp; LAG3 (NM_002286, 1289-1408), 120 bp; EGR2 (NM_000399, 590-711), 120 bp; β-actin (ACTB) (NM_001101, 411-511), 101 bp. Unknown quantities relative to the standard curve for a particular set of primers were calculated as previously reported (Endo et al., 2015), yielding the transcriptional quantitation of gene products relative to the endogenous standard, ACTB.

Measurement of IL-10 production by an enzyme-linked immunosorbent assay (ELISA)

Human IL-10 levels in culture supernatant samples were measured with a human IL-10 ELISA kit (Thermo Fisher Scientific), according to the manufacturer's protocol. Six hours after the treatments with $K_{Ca}3.1$ activators, culture medium was exchanged with new medium, and an additional 18 hr after the treatments, culture supernatant samples were collected.

Western blotting

Proteins lysates were prepared from HuT-78 cells using RIPA lysis buffer for Western blotting. Protein expression levels were measured 6 hr after the compound treatments. After the quantification of protein concentrations using the BIO-RAD DC™ protein assay, protein lysates were subjected to SDS-PAGE (10%). Blots were incubated with anti-Smad2/Smad3, anti-phospho-Smad2 (P-Smad2) (Ser465/467), anti-phospho-Smad3 (P-Smad3) (Ser423/425)

(Cell Signaling Technology Japan, Tokyo, Japan), and anti-ACTB (Medical & Biological Laboratories, Nagoya, Japan) antibodies, then incubated with anti-rabbit horseradish peroxidase-conjugated IgG (Merck, Darmstadt, Germany). An enhanced chemiluminescence detection system (Nacalai Tesque, Kyoto, Japan) was used to detect the bound antibody. The resulting images were analyzed using Amersham Imager 600 (GE Healthcare Japan, Tokyo, Japan). The light intensities of the Smad2/3, P-Smad2, and P-Smad3 protein band signals relative to that of the ACTB signal were calculated using ImageJ software (Ver. 1.42, NIH, Bethesda, MD, USA), and the respective ratios of P-Smad2/Smad2 and P-Smad3/Smad3 were obtained. In summarized results, relative protein expression levels in the vehicle control were expressed as 1.0.

Measurement of membrane potential and intracellular concentrations by a voltage-sensitive fluorescent dye and fluorescent Ca^{2+} indicator dye imaging

Membrane potential was measured using the fluorescent voltage-sensitive dye $DiBAC_4(3)$ as previously reported (Endo et al., 2015). Cells were seeded onto fibronectin-coated glass-bottomed dishes (Matsunami, Osaka, Japan). Briefly, prior to fluorescence measurements, HuT-78 cells were incubated in normal HEPES buffer containing 100 nM $DiBAC_4(3)$ at room temperature for 20 min, and then continuously incubated in 100 nM $DiBAC_4(3)$ throughout the experiments. In addition, intracellular Ca^{2+} concentrations were measured using the fluorescent Ca^{2+} indicator dye Fura 2-AM. Cells were incubated with 10 μM Fura 2-AM in normal HEPES solution for 30 min at room temperature. Cells loaded with Fura 2-AM were alternatively illuminated at wavelengths of 340 and 380 nm. Fluorescence images were recorded on the ORCA-Flash2.8 digital camera (Hamamatsu Photonics, Hamamatsu, Japan). Data collection and analyses were performed using an HCImage system (Hamamatsu Photonics). Images were measured every 5 sec.

Molecular Pharmacology Fast Forward. Published on January 8, 2019 as DOI: 10.1124/mol.118.114405
This article has not been copyedited and formatted. The final version may differ from this version.

Electrophysiological recording

A whole-cell patch clamp was applied to single HuT-78 cells using the CEZ-2400 amplifier (Nihon Kohden, Tokyo, Japan) at room temperature (23 ± 1ºC). The procedures used for electrophysiological recordings and data acquisition/analysis have been reported previously (Ohya et al., 2014). Membrane potential values and whole-cell current densities were measured in the current- and voltage-clamp modes, respectively. Whole-cell currents were induced by ramp depolarization from -120 to +60 mV, 200 msec duration, every 15 sec at +80 mV holding potential. The data were expressed as the current density (pA/pF). The external solution was (in mM): 137 NaCl, 2.2 KCl, 1.2 $MgCl_2$, 14 glucose, and 10 HEPES, pH7.4. The pipette solution was (in mM): 140 KCl, 4 $MgCl_2$, 3.2 $CaCl_2$, 5 EGTA, 10 HEPES, and 2 Na_2ATP, pH 7.2, with an estimated free Ca^{2+} concentration of 300 nM (pCa 6.5).

Confocal imaging of the nuclear translocation of P-Smad2 and P-Smad3

HuT-78 cells were fixed and permeabilized using the CytoFix/Perm kit (BD Pharmingen, Franklin Lakes, NJ, USA). Anti-P-Smad2 and anti-P-Smad3 antibodies were labeled with an Alexa Fluor 488-conjugated secondary antibody (Abcam, Cambridge, UK), and nuclei were labeled with DAPI. Fluorescence images were visualized using a confocal laser scanning microscope system (Nikon A1R, Tokyo, Japan) (Endo et al., 2015). Image data were quantitatively analyzed using ImageJ software.

Chemicals

DCEBIO (PubChem CID 656765) (Tocris Bioscience, Bristol, UK), SKA-31 (94880) (Sigma), $DiBAC_4(3)$ (6438341) (Dojin, Kumamoto, Japan), LY 364947 (447966) (Cayman Chemical, Ann Arbor, MI, USA), TRAM-34 (656734) (Santa Cruz Biotechnology, Dallas, TX, USA),

Molecular Pharmacology Fast Forward. Published on January 8, 2019 as DOI: 10.1124/mol.118.114405
This article has not been copyedited and formatted. The final version may differ from this version.

KN-62 (5312126) (MedChemexpress, Monmouth Junction, NJ, USA), UCL1684 (656733) (Tocris Bioscience), AZD 5363 (25227436) (Cayman Chemical), 5,15-DPP (diphenylporphyrin) (10895852) (Abcam), everolimus (6442177) (Cayman Chemical), and Bay 11-7082 (535343) (Sigma). All chemicals used in the present study were from Sigma-Aldrich, Wako Pure Chemical Industries, or Nacalai Tesque (Kyoto, Japan) unless otherwise stated.

Statistical analysis

The significance of differences among two and multiple groups was evaluated using the Student's or Welch's *t*-test and Tukey's test after the F test and ANOVA, respectively. Significance at $P < 0.05$ and $P < 0.01$ is indicated in the figures. Data are presented as the means ± S.D.

Molecular Pharmacology Fast Forward. Published on January 8, 2019 as DOI: 10.1124/mol.118.114405
This article has not been copyedited and formatted. The final version may differ from this version.

Results

Functional expression of $K_{Ca}3.1$ K^+ channels in IL-10-expressing HuT-78 cells

Previous studies showed that human T-cell lymphoma HuT-78 cells express the anti-inflammatory cytokine IL-10 at a relatively high level (Mori et al., 1997; Tiffon et al., 2011). HuT-78 cells strongly expressed IL-10 transcripts, but not Th1, Th2, or Th17 cytokine transcripts (IFN-γ, IL-17A, IL-4, IL-5, and IL-13) (Fig. S1A), whereas the other hematological cell lines (Jurkat E6, Daudi, K562, and THP-1) rarely expressed IL-10 (Fig. S1B). Concomitant with these results, IL-10 secretion was markedly higher in HuT-78 cells than in Jurkat E6, Daudi, K562, and THP-1 cells (Fig. S1C). A quantitative PCR assay showed that HuT-78 cells negatively expressed CD25 and Foxp3 (Fig. S1D). These results indicate that HuT-78 cells have a similar phenotype to $CD4^+CD25^-Foxp3^-$ inducible regulatory T (iTreg) cells. IL-10-producing $CD4^+CD25^-Foxp3^-$ iTreg cells express both the lymphocyte activation gene-3 (LAG3) and early growth response gene-2 (EGR2) (Okamura et al., 2009). HuT-78 cells expressed both genes at relatively high levels (Fig. S1D).

Among five Ca^{2+}-activated K^+ channel subtypes, $K_{Ca}3.1$ transcripts were the most abundantly expressed in HuT-78 cells (Fig. 1A). Additionally, among six $K_{Ca}3.1$ function-modifying molecules, NDPK-B, which enhances $K_{Ca}3.1$ activity, was the most abundantly expressed in HuT-78 cells (Fig. 1B). The depolarization responses induced by the $K_{Ca}3.1$ inhibitor, TRAM-34 (1 μM) were subsequently measured by voltage-sensitive fluorescent dye imaging. The application of TRAM-34 did not result in depolarization responses [$P > 0.05$ vs. vehicle control (0.1% DMSO)], suggesting that $K_{Ca}3.1$ is only activated under normal conditions in HuT-78 cells (Fig. 1C, 1D). On the other hand, the application of two different $K_{Ca}3.1$ activators (1 μM DCEBIO and 1 μM SKA-31) induced hyperpolarization responses ($P < 0.01$ vs. vehicle control) (Fig. 1C, 1D). An approximately 80% reduction in the DCEBIO-

Molecular Pharmacology Fast Forward. Published on January 8, 2019 as DOI: 10.1124/mol.118.114405
This article has not been copyedited and formatted. The final version may differ from this version.

induced hyperpolarization response was observed following the application of TRAM-34 (1 μM) (not shown). 1 μM SKA-31-induced activation of $K_{Ca}3.1$ was also observed using the whole-cell patch clamp recordings. In current-clamp mode, the magnitude of membrane hyperpolarization by 1 μM SKA-31 was -69.6 ± 2.3 mV (n=5, $P < 0.01$ vs. vehicle) (Fig. S2A, S2B). In voltage-clamp mode, the currents induced by ramp depolarization from -120 mV to +60 mV were activated by the application of 1 μM SKA-31 (Fig. S2C), and the current density at +60 mV in SKA-31-treated cells (286.9 ± 97.6 pA/pF, n=7, $P < 0.05$) was larger than vehicle control (170.3 ± 95.0 pA/pF, n=7) (Fig. S2C, S2D). Both SKA-31-induced hyperpolarization and current activation were suppressed following the application of 1 μM TRAM-34 (Fig. S2A, S2C). The application of $K_{Ca}3.1$ activators induced hyperpolarization-induced intracellular Ca^{2+} elevation (Fig. 1E, 1F). The elevated Ca^{2+} levels ($\Delta ratio_{340/380}$) were 0.017 ± 0.017 (n=28), 0.063 ± 0.042 (n=22, $P < 0.01$), and 0.052 ± 0.044 (n=35, $P < 0.01$) in vehicle-, DCEBIO-, and SKA-31-treated cells, respectively.

Inhibitory effects of $K_{Ca}3.1$ activators on IL-10 gene expression and production in HuT-78 cells

Using IL-10-producing HuT-78 cells that functionally expressed $K_{Ca}3.1$ K^+ channels, we examined the effects of $K_{Ca}3.1$ activators on IL-10 transcription and secretion. As shown in Figures 2A and 2C, IL-10 transcription and secretion were both reduced by the treatments with 1 μM DCEBIO and 1 μM SKA-31. The expression levels of IL-10 transcripts relative to ACTB were 0.039 ± 0.002, 0.019 ± 0.002, and 0.025 ± 0.002 in vehicle-, DCEBIO-, and SKA-31-treated HuT-78 cells, respectively (n=4 for each, $P < 0.01$ vs. vehicle control). The expression levels of vehicle-treated cells is arbitrarily expressed as 1.0. We further examined the effects of 30 mM K^+-induced depolarization on $K_{Ca}3.1$ activators-induced inhibition of IL-10 transcription in HuT-78 cells. The application of 30 mM K^+-containing solution induced the

moderate depolarization in HuT-78 cells (Fig. S3A). Similar to the results in Fig. 1C, 1 μM SKA-31 induced obvious hyperpolarization responses under normal K^+ (2.2 mM) concentration, however, they were almost disappeared by 30 mM K^+-containing solution (Fig. S3B). Concomitant with these results, $K_{Ca}3.1$ activators-induced inhibitions of IL-10 transcription disappeared by 30 mM K^+-containing solution (Fig. S3C). In addition, the treatment with the Ca^{2+}-ATPase inhibitor, thapsigargin (TG, 1 nM) for 6 hr reduced IL-10 transcription (Fig. S3D). IL-10 secretion levels (6 to 24 hr) were 3207 ± 22, 2206 ± 168, and 2321 ± 66 pg/mL in vehicle-, DCEBIO-, and SKA-31-treated HuT-78 cells, respectively (n=4 for each, $P < 0.01$ vs. vehicle control) (Fig. 2B). Approximately 20% of IL-10 secretion was inhibited by the treatments with $K_{Ca}3.1$ activators in HuT-78 cells. The transcriptional repression of IL-10 was not found 1 or 3 hr after the treatments with $K_{Ca}3.1$ activators (Fig. S4), and no changes in IL-10 secretion levels were observed in the culture medium from HuT-78 cells treated with vehicle, DCEBIO, and SKA-31 for 0 to 6 hr: 961 ± 62, 877 ± 114, and 872 ± 66 pg/mL, respectively (n=4 for each, $P > 0.05$ vs. vehicle control). Consistent with the results shown in Figures 2C and 2D, no changes in the expression levels of IL-10 transcripts were noted following the treatment with 1 μM TRAM-34 for 6 hr: 0.038 ± 0.008 relative to ACTB (n=4, $P > 0.05$ vs. vehicle control: 0.037 ± 0.004). When cells were pre-treated with 1 μM TRAM-34 for 5 min, reductions in IL-10 transcription and secretion by the treatments with $K_{Ca}3.1$ activators were mostly prevented (Fig. 2B, 2D). These results indicate that $K_{Ca}3.1$ is one of the molecules controlling IL-10 production in T-cell lymphoma.

Involvement of the Smad2/3 signaling pathway in $K_{Ca}3.1$ activator-induced transcriptional repression of IL-10 in HuT-78 cells

As shown in Figures 2A, S4B, and S4C, IL-10 transcription was inhibited by $K_{Ca}3.1$ activation within 6 hr. These results suggest that the $K_{Ca}3.1$ activator-induced transcriptional repression

of IL-10 is elicited through an IL-10 transcription factor-independent pathway. No changes in the transcriptional expression levels of the IL-10 transcription factors, E4BP4, GATA3, cMAF, and Blimp1, were found in HuT-78 cells (Fig. 3). Their expression levels to ACTB were 0.006 ± 0.001, 0.080 ± 0.010, 0.004 ± 0.001, and 0.014 ± 0.004, respectively, in vehicle-treated HuT-78 cells (n=4 for each). Kitani et al. (2003) showed that TGF-β1/Smad signaling positively regulated IL-10 gene expression in Th1 cells. Therefore, we assessed the expression levels of phosphorylated Smad2 (P-Smad2) and Smad3 (P-Smad3) by Western blotting. As shown in Figure 4A and Figure S5A, decreases in P-Smad2 proteins, but not P-Smad3 were found in $K_{Ca}3.1$ activator-treated (for 6 hr) HuT-78 cells, without changes in total Smad2 and Smad3 protein expression. After the ratios of P-Smad2/3 to total Smad2/3 were calculated in vehicle-, DCEBIO-, and SKA-31-treated HuT-78 cells, those in the vehicle control were expressed as 1.0. The relative expression of P-Smad2, but not Smad3 in DCEBIO- and SKA-31-treated HuT-78 cells was reduced (n=5 for each, $P < 0.01$) (Fig. 4B, 4C). In addition, P-Smad2 and P-Smad3 proteins were expressed in vehicle-treated HuT-78 cells, suggesting that Smad2 and Smad3 are constitutively active and TGF-β1-independently regulated in HuT-78 cells. The gene expression of IL-10 was not reduced by the treatment with the potent TGF-β1 receptor blocker, LY36497 (1 μM) (Fig. S6A).

In order to clarify whether $K_{Ca}3.1$ activators inhibit the nuclear translocation of P-Smad2 and/or P-Smad3 in HuT-78 cells, the cellular localization of P-Smad2/P-Smad3 was visualized by laser-scanning confocal fluorescence microscopy. Anti-P-Smad2 and anti-P-Smad3 antibodies were labeled with an Alexa Fluor 488-conjugated secondary antibody, and nuclei were labeled with DAPI (Fig. 5A). When the mean fluorescence intensities of the nuclear-cytoplasmic ratios of P-Smad2 and P-Smad3 were calculated, the nuclear translocation of P-Smad2, but not P-Smad3 was reduced by the treatments with $K_{Ca}3.1$ activators ($P < 0.01$) (Fig. 5B, 5C). These results suggest that the nuclear translocation of P-Smad2 is regulated by the

Molecular Pharmacology Fast Forward. Published on January 8, 2019 as DOI: 10.1124/mol.118.114405
This article has not been copyedited and formatted. The final version may differ from this version.

Ca^{2+}-dependent $K_{Ca}3.1$ downstream signaling pathway(s), and, thus, IL-10 as a target gene of Smad2/3 signaling may be transcriptionally regulated in HuT-78 cells.

Effects of the Ca^{2+}/calmodulin-dependent protein kinase II inhibitor on the $K_{Ca}3.1$ activator-induced inhibition of IL-10 expression and secretion, P-Smad2 protein expression, and the nuclear translocation of P-Smad2 in HuT-78 cells

Ca^{2+}/calmodulin-dependent protein kinase (CaMKII) blocks the nuclear accumulation of Smad2 and prevents Smad2-Smad3 interactions (Zimmerman et a., 1998; Wicks et al., 2000). Increases in intracellular Ca^{2+} concentrations through $K_{Ca}3.1$ activation enhance the CaMKII signaling pathway. Therefore, we investigated whether a pre-treatment with the CaMKII inhibitor, KN-62 (10 μM) for 1 hr prevents 1) the $K_{Ca}3.1$ activator-induced inhibition of IL-10 transcription and secretion, 2) P-Smad2 protein expression, and 3) the nuclear translocation of P-Smad2 in HuT-78 cells. In Figure 2A and 2C, $K_{Ca}3.1$ activators inhibited IL-10 transcription and secretion. As shown in Figure 6, the $K_{Ca}3.1$ activator-induced inhibition of them disappeared following the pre-treatment with KN-62 in HuT-78 cells. The expression levels of IL-10 transcripts were 0.035 ± 0.004, 0.040 ± 0.002, and 0.040 ± 0.002 relative to ACTB in vehicle-, DCEBIO-, and SKA-31-treated groups, respectively (n=4 for each, $P > 0.05$ vs. vehicle control). Thapsigargin (TG, 1 nM)-induced inhibition of IL-10 transcription also disappeared following the pre-treatment with KN-62 (Fig. S3D). In Figure 4, 5, $K_{Ca}3.1$ activators decreased the protein expression of P-Smad2 and the nuclear translocation of P-Smad2. $K_{Ca}3.1$ activator-induced decreases in them were both prevented by the pre-treatment with KN-62 in HuT-78 cells (Fig. 7, 8, S5B). These results suggest that CaMKII is an important mediator to promote the $K_{Ca}3.1$ activator-induced blockade of IL-10 transcription and secretion by suppressing the nuclear translocation of P-Smad2.

Molecular Pharmacology Fast Forward. Published on January 8, 2019 as DOI: 10.1124/mol.118.114405
This article has not been copyedited and formatted. The final version may differ from this version.

Discussion

The intermediate-conductance Ca^{2+}-activated K^+ channel $K_{Ca}3.1$ plays an important role in the control of pro-inflammatory cytokine production and secretion by regulating Ca^{2+} signaling in lymphoid and myeloid cells (Di et al., 2010; Ohya et al., 2014); however, it currently remains unclear whether $K_{Ca}3.1$ contributes to IL-10-induced escape from cancer immune surveillance. The present study showed that the pharmacological blockade of $K_{Ca}3.1$ by 1 μM TRAM-34 did not evoke depolarization responses in human T-cell lymphoma HuT-78 cells under resting conditions (Fig. 1C, 1D). These results suggest that $K_{Ca}3.1$ is rarely active under resting conditions in HuT-78 cells. In support of this hypothesis, IL-10 transcription was not affected by a single treatment with TRAM-34; however, TRAM-34 blocked $K_{Ca}3.1$ activator-induced decreases in IL-10 expression and secretion (Fig. 2B, 2D). Using a whole-cell patch clamp recording in current- and voltage-clamp modes, SKA-31-induced hyperpolarization and current activation were almost completely inhibited following the application of 1 μM TRAM-34 (Fig. S2). The main results of the present study are: 1) the IL-10 expression and secretion were inhibited in HuT-78 cells treated with $K_{Ca}3.1$ activators (Fig. 2), 2) $K_{Ca}3.1$ activators reduced the phosphorylation of Smad2 and its nuclear translocation in HuT-78 cells (Fig. 4, 5), resulting in the partial inhibition of constitutively active Smad2/3 signaling, and 3) the pharmacological inhibition of CaMKII signaling prevented the $K_{Ca}3.1$ activator-induced transcriptional repression of IL-10 through the re-activation of constitutive active Smad2/3 signaling (Fig. 6, 7, 8). This is the first evidence to suggest that $K_{Ca}3.1$ activators are a novel therapeutic option to suppress the tumor-promoting activities of IL-10 in escape from cancer immune surveillance.

During the last decade or two, several transcription factors of IL-10 have been identified in immune cells: E4BP4, GATA3, cMAF, and Blimp1 (Shoemaker et al., 2006; Motomura et al., 2011; Male et al., 2012; Heinemann et al., 2014; Rutz & Ouyang, 2016; Xu et al., 2018).

Molecular Pharmacology Fast Forward. Published on January 8, 2019 as DOI: 10.1124/mol.118.114405
This article has not been copyedited and formatted. The final version may differ from this version.

As shown in Figure 3, no changes in the expression levels of these transcripts by the treatments with $K_{Ca}3.1$ activators for 6 hr were found in HuT-78 cells ($P > 0.05$). Priceman et al. (2006) reported that the expression level of E4BP4 was regulated in a Ca^{2+}-dependent manner in human leukemic cells; however, it was not affected by longer treatments with $K_{Ca}3.1$ activators for 12 and 24 hr (not shown). Alternatively, the pro-inflammatory cytokine, IL-32, which is detected in sera from patients with Crohn's disease and rheumatoid arthritis, increases IL-10 transcription (Kang et al., 2009). In HuT-78 cells, IL-32 transcripts were expressed at a high level (approximately 10-fold that of IL-10); however, no changes were observed in their expression levels following treatments with $K_{Ca}3.1$ activators for 6 hr: 0.39 ± 0.02, 0.48 ± 0.08, and 0.40 ± 0.16 relative to ACTB in vehicle-, DCEBIO-, and SKA-31-treated HuT-78 cells (n=4 for each, $P > 0.05$ vs. vehicle control). A recent study showed that IL-10 transcription is epigenetically regulated in immune cells, and histone deacetylase 11 (HDAC11) is a possible candidate for the transcriptional repression of IL-10 (Yanginlar & Logie, 2017). However, the expression levels of HDAC11 transcripts were extremely low in HuT-78 cells (less than 0.0001 relative to ACTB) (not shown). These results suggest that these transcriptional and post-translational modulators are not involved in the $K_{Ca}3.1$ activator-induced transcriptional repression of IL-10.

Recent studies showed that $K_{Ca}3.1$ blockade attenuated pulmonary, renal, and corneal fibrosis by mediating Smad2/3 signaling (Huang et al., 2013; Roach & Wulff, 2014; Roach et al., 2015; Anumanthan et al., 2018; Huang 2018). The resultant decreases in Ca^{2+} influx prevented the phosphorylation of Smad2/3 and nuclear translocation of P-Smad2/3 in fibroblasts, and, thus, the expression levels of the downstream target genes, α-smooth muscle actin, α-SMA, and collagen type I, were decreased. These results indicate that $K_{Ca}3.1$ is a 'positive' regulator of Smad2/3 signaling in fibroblasts. In fibroblasts from patients with idiopathic pulmonary fibrosis, Ca^{2+}- and $K_{Ca}3.1$-dependent processes contribute to the

constitutive activation of Smad2/3 signaling (Roach et al. 2014 & 2015). Mukherjee et al. (2017) showed that CaMKII activation did not affect Smad2/3 signaling in fibroblasts. However, the present study showed that K_{Ca}3.1 functioned as a 'negative' regulator of Smad2/3 signaling through CaMKII in HuT-78 cells (Fig. 6-8). In HuT-78 cells, constitutively active NF-κB contributes to the constitutive facilitation of Smad2/3 signaling (Mori et al., 1997; Tiffon et al., 2011); however, resting K_{Ca}3.1 activity was very low (Fig. 1C, 1D). Consistent with our results, previous studies reported that the inhibition of Smad2/3 signaling was strongly dependent on CaMKII activation, and CaMKII blocked the nuclear accumulation of Smad2 and prevented Smad2-Smad3 interactions (Zimmerman et al., 1998; Wicks et al., 2000). The present results provide novel evidence to suggest that K_{Ca}3.1 activators successfully inhibit constitutively active Smad2/3 signaling via CaMKII activation in IL-10-producing tumor-infiltrating lymphocytes and lymphoma.

STAT3 and PI3K/AKT/mTOR signaling pathways are both involved in the regulation of IL-10 expression (Braunschweig et al., 2011;Male et al., 2012; Zhu et al., 2015; Huang et al., 2016). STAT-3 and mTOR inhibition reduced IL-10 expression in natural killer cells (Male et al., 2012) and peripheral dendritic cells (Weichhart et al., 2008), respectively. K_{Ca}3.1 blockade has been shown to inhibit the TGF-β1 signaling pathway through PI3K/AKT/mTOR signaling pathways (Huang et al., 2016), while PI3K/AKT/mTOR signaling positively and negatively regulated STAT3 and NF-κB, respectively (Weichhart et al., 2008). Furthermore, a positive feedback loop may operate to maintain strong STAT3 activity and IL-10 expression. IL-10 expression was reduced by the treatment with the NF-κB inhibitor, Bay 11-7082 (1 μM) (Fig. S6B); however, no changes were observed in its expression following a treatment with the STAT3 inhibitor, 5,15-DPP (20 μM), the mTOR inhibitor, everolimus (10 nM), and the AKT inhibitor, AZD 5363 (1 μM) for 6 (Fig. S6C), 12, and 24 hr (not shown) in HuT-78 cells. These

Molecular Pharmacology Fast Forward. Published on January 8, 2019 as DOI: 10.1124/mol.118.114405
This article has not been copyedited and formatted. The final version may differ from this version.

results suggest that STAT3 and PI3K/AKT/mTOR signaling pathways do not play an essential role in $K_{Ca}3.1$ activator-induced transcriptional repression in HuT-78 cells.

In conclusion, the present study provided a new approach to IL-10 regulation in cancer immunotherapy. The results obtained clearly showed that IL-10 is a downstream gene of Smad2/3 signaling in HuT-78 cells, and its production is negatively regulated by $K_{Ca}3.1$ activation, which blocks the nuclear accumulation of constitutively active Smad2 through CaMKII signaling. $K_{Ca}3.1$ activators are a possible therapeutic option to suppress the tumor-promoting activities of IL-10.

Molecular Pharmacology Fast Forward. Published on January 8, 2019 as DOI: 10.1124/mol.118.114405
This article has not been copyedited and formatted. The final version may differ from this version.

Acknowledgments

We sincerely thank Motoki Shimozawa and Mayu Fujimoto for their technical assistance. Medical English Service (Kyoto, Japan) reviewed the manuscript prior to its submission.

Authorship contributions

Participated in research design: Matsui, Ohya

Conducted experiments: Matsui, Kajikuri, Kito, Endo, Hasegawa, Murase, Ohya

Performed data analysis: Matsui, Kajikuri, Kito, Endo, Hasegawa, Murase, Ohya

Wrote or contributed to the writing of the manuscript: Matsui, Kajikuri, Kito, Ohya

References

Alotaibi MR, Hassan ZK, Al-Rejaie SS, Alshammari MA, Almutairi MM, Alhoshani AR, Alanazi WA, Hafez MM, and Al-Shabanah OA (2018) Characterization of apoptosis in a breast cancer cell line after IL-10 silencing. *Asian Pac J Cancer Prev* **19:** 777-783.

Anumanthan G, Gupta S, Fink MK, Hesemann NP, Bowies DK, McDaniel LM, Muhammad M, and Mohan RR (2018) KCa3.1 ion channel: A novel therapeutic target for corneal fibrosis. *PLoS One* **13:** e0192145.

Benjamin D, Knobloch TJ, and Dayton MA (1992) Human B-cell interleukin10: B-cell lines derived from patients with acquired immunodeficiency syndrome and Burkitt7s lymphoma constitutively secrete large quantities of interleukin-10. *Blood* **80:** 1289-1298.

Blay JY, Burdin N, Rousset F, Lenoir G, Biron P, Philip T, Banchereau J, and Favrot MC (1993) Serum interleukin-10 in non-Hodgkin's lymphoma: a prognostic factor. *Blood* **82:** 2169-2174.

Braunschweig A, Poehlmann TG, Busch S, Schleussner E, and Markert UR (2011) Signal transducer and activator of transcription 3 (STAT3) and suppressor of cytokine signaling (SOCS3) balance controls cytotoxicity and IL-10 expression in decidual-like natural killer cell line NK-92. *Am J Reprod Immunol* **66:** 329-335.

Burugu S, Gao D, Leung S, Chia SK, and Nielsen TO (2017) $LAG3^+$ tumor infiltrating lymphocytes in breast cancer: clinical correlates and association with PD-1/$PD\text{-}L1^+$ tumors. *Ann Oncol* **28:** 2977-2984.

Cahalan MD and Chandy KG (2009) The functional network of ion channels in T lymphocytes. *Immunol Rev* **231:** 59-87.

Classen S, Zander T, Eggle Z, Chemnitz JM, Brors B, Buchmann I, Popov A, Beyer M, Eils R, Debey S, and Schultze JL (2007) Human resting $CD4^+$ T cells are constitutively inhibited by TGFβ under steady-state conditions. *J Immunol* **178:** 6931-6940.

Derynck R and Zhang YE (2003) Smad-dependent and Smad-independent pathways in TGF-β family signaling. *Nature* **425:** 577-584.

Di L, Srivastava S, Zhdanova O, Ding Y, Li Z, Wulff H, Lafaille M, and Skolnik EY (2010) Inhibition of the K^+ channel KCa3.1 ameliorates T cell-mediated colitis. *Proc Natl Acad Sci U S A* **107:** 1541-1546.

Eil R, Vodnala SK, Clever D, Klebanoff CA, Sukumar M, Pan JH, Palmer DC, Gros A, Yamamoto TN, Patel SJ, Guittard GC, Yu Z, Carbonaro V, Okkenhaug K, Schrump DS, Linehan WM, Roychoudhuri R, and Restifo NP (2016) Ionic immune suppression within the tumour microenvironment limits T cell effector function. *Nature* **537:** 539-543.

Endo K, Kurokawa N, Kito N, Nakakura S, Fujii M, and Ohya S (2015) Molecular identification of the dominant-negative, splicing isoform of the two-pore domain K^+ channel $K_{2P}5.1$ in lymphoid cells and enhancement of its expression by splicing inhibition. *Biochem Pharmacol* **98:** 440-452.

Feske S, Wulff H, and Skolnik EY (2015) Ion channels in innate and adaptive immunity. *Annu Rev Immunol* **33:** 291-353.

Finke J, Ternes P, Lange W, Mertelsmann R, and Dölken G (1993) Expression of interleukin 10 in B lymphocytes of different origin. *Leukemia* **7:** 1852-1857.

Hamidullah, Changkija B, and Konwar R (2012) Role of interleukin-10 in breast cancer. *Breast Cancer Res Treat* **133:** 11-21.

Heinemann C, Heink S, Petermann F, Vasanthakumar A, Rothhammer V, Doorduijn E, Mitsdoerffer M, Sie C, Prazeres Da Costa O, Buch T, Hemmer B, Oukka M, Kallies A,

and Korn T (2014) IL-27 and IL-12 oppose pro-inflammatory IL-23 in $CD4^+$ T cells by inducing Blimp1. *Nat Commun* **5:** 3770.

Huang C, Lin MZ, Cheng D, Breat F, Pollock CA, and Chen XM (2016) KCa3.1 mediates dysfunction of tubular autophagy in diabetic kidneys via PI3K/Akt/mTOR signaling pathways. *Sci Rep* **6:** 23884.

Huang C, Shen S, Ma Q, Chen J, Gill A, Pollock CA, and Chen XM (2013) Blockade of KCa3.1 ameliorates renal fibrosis through the TGF-β1/Smad pathway in diabetic mice. *Diabetes* **62:** 2923-2934.

Huang C, Shen S, Ma Q, Gill A, Pollock CA, and Chen XM (2018) The KCa3.1 blocker TRAM-34 reverses renal damage in a model of established diabetic nephropathy. *PLoS One* **13:** e0192800.

Itoh M, Takahashi T, Sakaguchi N, Kuniyasu Y, Shimizu J, Otsuka F, and Sakaguchi S (1999) Thymus and autoimmunity: production of $CD25^+CD4^+$ naturally anergic and suppressive T cells as a key function of the thymus in maintaining immunologic self-tolerance. *J Immunol* **162:** 5217-5326.

Kang JW, Choi SC, Cho MC, Kim HJ, Kim JH, Lim JS, Kim SH, Han JY, and Yoon DY (2009) A proinflammatory cytokine interleukin-32β promotes the production of an anti-inflammatory cytokine interleukin-10. *Immunology* **128:** e532-e540.

Kitani A, Fuss I, Nakamura K, Kumaki F, and Usui T (2003) Transforming growth factor (TGF)-β1-producing regulatory T cells induce Smad-mediated interleukin 10 secretion that facilitates coordinated immunoregulatory activity and amelioration of TGF-β1-mediated fibrosis. *J Exp Med* **198:** 1179-1188.

Kuras Z, Yun YH, Chimote AA, Neumeier L, and Conforti L (2012) $K_{Ca}3.1$ and TRPM7 channels at the uropod regulate migration of activated human T cells. *PLoS One* **7:** e43859.

Lu ZY, Zhang XG, Rodriguez C, Wijdenes J, Gu ZJ, Morel-Fournier B, Harousseau JL, Bataille R, Rossi JF, and Klein B (1995) Interleukin-10 is a proliferation factor but not a differentiation factor for human myeloma cells. *Blood* **85:** 2521-2527.

Ma QY, Huang DY, Zhang HJ, Wang S, and Chen XF (2017) Function and regulation of LAG3 on $CD4^+CD25^-$ T cells in non-small cell lung cancer. *Exp Cell Res* **360:** 358-364.

Male V, Nisolo I, Gascoyne DM, and Brady HJ (2012) E4BP4: an unexpected player in the immune response. *Trends Immunol* **33:** 98-102.

Ming M, Manzini I, Le W, Krieglstein K, and Spittau B (2010) Thapsigargin-induced Ca^{2+} increase inhibits TGFβ1-mediated Smad2 transcription responses via Ca^{2+}/calmodulin-dependent protein kinase II. *J Cell Biochem* **111:** 1222-1230.

Mori N and Prager D (1997) Activation of the lnterleukin-10 gene in the human T lymphoma line HuT 78: identification and characterization of NF-κB binding sites in the regulatory region of the interleukin-10 gene. *Eur J Hematol* **59:** 162-170.

Motomura Y, Kitamura H, Hijikata A, Matsunaga Y, Matsumoto K, Inoue H, Atarashi K, Hori S, Watarai H, Xhu J, Taniguchi M, and Kubo M (2011) The transcription factor E4BP4 regulates the production of IL-10 and IL-13 in $CD4^+$ T cells. *Nat Immunol* **12:** 450-459

Mukherjee S, Sheng W, Sun R, and Janssen LJ (2017) Ca^{2+}/calmodulin-dependent protein kinase IIβ and IIδ mediate TGFβ-induced transduction of fibronectin and collagen in human pulmonary fibroblasts. *Am J Physiol Lung Cell Mol Physiol* **312:** L510-L519.

Ohya S and Kito H (2018) Ca^{2+}-activated K^+ channel $K_{Ca}3.1$ as a therapeutic target for immune disorders. *Biol Pharm Bull* **41:** 1158-1163.

Ohya S, Fukuyo Y, Kito H, Shibaoka R, Matsui M, Niguma H, Maeda Y, Yamamura H, Fujii M, Kimura K, and Imaizumi Y (2014) Upregulation of $K_{Ca}3.1$ K^+ channel in mesenteric lymph node $CD4^+$ T lymphocytes for a mouse model of dextran sodium sulfate-induced inflammatory bowel disease. *Am J Physiol Gastrointest Liver Physiol* **306:** G873-G88.

Okamura T, Fujio K, Shibuya M, Sumitomo S, Shoda H, Sakaguchi S, and Yamamoto K (2009) $CD4^+CD25^-LAG3^+$ regulatory T cells controlled by the transcription factor Egr-2. *Proc Natl Acad Sci U S A* **106:** 13974-13979.

Priceman SJ, Kirzner JD, Nary LJ, Morris D, Shankar DB, Samamoto KM, and Medh RD (2006) Calcium-dependent upregulation of E4BP4 expression correlates with glucocorticoid-evoked apoptosis of human leukemic CEM cells. *Biochem Biophys Res Commun* 344: 491-499.

Roach KM, Feghali-Bostwich C, Wulff H, Amrani Y, and Bradding P (2015) Human lung myofibroblast TGF-β1-dependent Smad2/3 signaling is Ca^{2+}-dependent and regulated by $K_{Ca}3.1$ K^+ channels. *Fibrogenesis Tissue Repair* **8:** 5.

Roach KM, Wulff H, Feghali-Bostwick C, Amrani Y, and Bradding P (2014) Increased constitutive αSMA and Smad2/3 expression in idiopathic pulmonary fibrosis myofibroblasts is $K_{Ca}3.1$-dependent. *Respir Res* **15:** 155.

Rutz S and Ouyang W (2016) Regulation of interleukin-10 expression. *Adv Exp Med Biol* **941:** 89-116.

Sato T, Terai M, Tamura Y, Alexeev V, Mastrangelo MJ, and Selvan SR (2011) Interleukin 10 in the tumor microenvironment: a target for anticancer immunotherapy. *Immunol Res* **51:** 170-182.

Sekiya T, Nakatsukasa H, Lu Q, and Yoshimura A (2016) Roles of transcription factors and epigenetic modifications in differentiation and maintenance of regulatory T cells. *Microbes Infect* 18: 378-386.

Shoemaker J, Saraiva M, and O'Garra A (2006) GATA-3 directly remodels the IL-10 locus independently of IL-4 in $CD4^+$ T cells. *J Immunol* **176:** 3470-3479.

Tiffon CE, Adams JE, van der Fits L, Wen S, Townsend PA, Ganesan A, Hodges E, Vermeer MH, and Packham G (2011) The histone deacetylase inhibitors vorinostat and romidepsin

downmodulate IL-10 expression in cutaneous T-cell lymphoma cells. *Br J Pharmacol* **162:** 1590-1602.

Weichhart T, Costantino G, Poglitsch M, Rosner M, Zeyda M, Stuhlmeier KM, Kolbe T, Stulnig TM, Hörl WH. Hengstschläger M, Müller M, and Säemann MD (2008) The TSC-mTOR signaling pathway regulates the innate inflammatory response. *Immunity* **29:** 565-577.

Wicks SJ, Lui S, Abdel-Wahab M, Mason RM, and Chantry A (2000) Inactivation of smad-transforming growth factor beta signaling by Ca^{2+}-calmodulin-dependent protein kinase II. *Mol Cell Biol* **20:** 8103-8111.

Xu M, Pokrovskii M, Ding Y, Yi R, Au C, Harrison OJ, Galan C, Belkaid Y, Bonneau R, and Littmann DR (2018) c-MAF-dependent regulatory T cells mediate immunological tolerance to a gut pathobiont. *Nature* **554:** 373-377.

Yanginlar C and Logie C (2017) HDAC11 is a regulator of diverse immune functions. *Biochim Biophys Acta* **1861:** 54-49.

Zhu YP, Brown JR, Sag D, Zhang L, and Suttles J (2015) Adenosine 5'-monophosphate-activated protein kinase regulates IL-10-mediated anti-inflammatory signaling pathways in macrophages. *J Immunol* **194:** 584-494.

Zimmerman CM, Kariapper MST, and Mathews LS (1998) Smad proteins physically interact with calmodulin. *J Biol Chem* **278:** 677-680.

Molecular Pharmacology Fast Forward. Published on January 8, 2019 as DOI: 10.1124/mol.118.114405
This article has not been copyedited and formatted. The final version may differ from this version.

Footnotes

This work was supported by JSPS KAKENHI Grant number [JP16K08285] (S.O.). The authors declare no conflict of interest.

Figure legends

Figure 1. Functional expression of $K_{Ca}3.1$ K^+ channels in HuT-78 cells. A, B: Real-time PCR assay for K_{Ca} channel subtypes ($K_{Ca}1.1$, $K_{Ca}2.x$, and $K_{Ca}3.1$) (A) and $K_{Ca}3.1$ function-modifying molecules (PI3K-C2B, NDPK-B, PHPT1, MTMR6, PGAM5, and TRIM27) (B) (n=4 for each). Expression levels were expressed as a ratio to ACTB. C: The time course of changes in the relative fluorescent intensity of $DiBAC_4(3)$ by the application of $K_{Ca}3.1$ activators (1 μM DCEBIO and 1 μM SKA-31) and a $K_{Ca}3.1$ inhibitor (1 μM TRAM-34). The fluorescent intensity of $DiBAC_4(3)$ before the application of the agents at 0 sec is expressed as 1.0. Horizontal bar shows the duration of drug application. D: Summarized data are shown as Δ relative fluorescence intensity in vehicle (0.01% DMSO)-, TRAM-34-, DCEBIO-, and SKA-31-treated HuT-78 cells. E: The time course of changes in the intracellular Ca^{2+} concentration ($[Ca^{2+}]_i$) by the application of $K_{Ca}3.1$ activators. $[Ca^{2+}]_i$ was expressed as the Fura-2 ratio (340 nm/380 nm). F: Summarized data are shown as Δ Fura-2 ratio (340 nm/380 nm) in vehicle-, DCEBIO-, and SKA-31-treated HuT-78 cells. Cell numbers used for the experiments are shown in parentheses. Results are expressed as means ± S.D. **: $P < 0.01$ vs. vehicle control.

Figure 2. Effects of treatments with $K_{Ca}3.1$ activators on IL-10 transcription and secretion in HuT-78 cells. A, B: Quantitative real-time PCR assay for IL-10 in HuT-78 cells treated with vehicle, DCEBIO (1 μM), and SKA-31 (1 μM) for 6 hr in the absence [TRAM-34 (-)] and presence [TRAM-34 (+)] of TRAM-34 (1 μM) (n=4 for each). The expression levels of vehicle-treated cells is arbitrarily expressed as 1.0, and data are shown as "relative expression". C, D: Quantitative detection of IL-10 by an ELISA assay in HuT-78 cells treated with vehicle, DCEBIO, and SKA-31 for 18 hr (see 'Materials and Methods) in the absence (C) and presence (D) of TRAM-34. Results are expressed as means ± S.D. **: $P < 0.01$ vs. vehicle control.

Molecular Pharmacology Fast Forward. Published on January 8, 2019 as DOI: 10.1124/mol.118.114405
This article has not been copyedited and formatted. The final version may differ from this version.

Figure 3. Effects of treatments with $K_{Ca}3.1$ activators on the expression levels of transcription factors of IL-10 in HuT-78 cells. A-D: Quantitative real-time PCR assay for transcription factors of IL-10, E4BP4 (A), GATA3 (B), cMAF (C), and Blimp1 (D) in HuT-78 cells treated with vehicle, DCEBIO (1 μM), and SKA-31 (1 μM) for 6 hr (n=4 for each). The expression levels of vehicle-treated cells is arbitrarily expressed as 1.0, and data are shown as "relative expression". Results are expressed as means ± S.D.

Figure 4. Effects of treatments with $K_{Ca}3.1$ activators for 6 hr on the phosphorylation of Smad2 and Smad3 proteins in HuT-78 cells. A: Whole protein lysates of DCEBIO (1 μM) and SKA-31 (1 μM)-treated HuT-78 cells were probed by immunoblotting with anti-Smad2/Smad3 (a, upper panel), anti-phospho-Smad2 (P-Smad2) (b, upper panel), anti-P-Smad3 (c, upper panel), and anti-ACTB antibodies (a-c, lower panels). B, C: Summarized results of the relative expression of P-Smad2/Smad2 and P-Smad3/Smad3 were obtained from the optical density of Smad2/3, P-Smad2, P-Smad3, and ACTB band signals (n=5 for each) (see Materials and Methods). Results are expressed as means ± S.D. **: $P < 0.01$ vs. vehicle control.

Figure 5. Effects of treatments with $K_{Ca}3.1$ activators for 6 hr on the nuclear translocation of P-Smad2 and P-Smad3 in HuT-78 cells. A: Confocal fluorescent images of Alexa Fluor 488-labeled P-Smad2 and P-Smad3 in vehicle-, DCEBIO (1 μM)-, and SKA-31 (1 μM)-treated HuT-78 cells. Nuclear morphologies were shown by DAPI images. Thick and thin dashed lines showed the nuclear boundary and the plasma membrane, respectively. B, C: Summarized results of the expression levels of P-Smad2 (B) and P-Smad3 (C) in the nuclei of HuT-78 cells. The mean fluorescent intensities of nuclear-cytoplasmic ratios were calculated. Results are

expressed as means ± S.D. Cell numbers used for the experiments are shown in parentheses. **: $P < 0.01$ vs. vehicle control.

Figure 6. Effects of the CaMKII inhibitor, KN-62 (10 μM) on $K_{Ca}3.1$ activator-induced reductions in IL-10 transcription and secretion in HuT-78 cells. A: Quantitative real-time PCR assays for IL-10 in HuT-78 cells treated with vehicle, DCEBIO (1 μM), and SKA-31 (1 μM) for 6 hr in the presence of KN-62 (n=4 for each). The expression levels of vehicle-treated cells is arbitrarily expressed as 1.0, and data are shown as "relative expression". B: Quantitative detection of IL-10 by ELISA assays in HuT-78 cells treated with vehicle, DCEBIO, and SKA-31 for 18 hr in the presence of KN-62. Results are expressed as means ± S.D.

Figure 7. Effects of the CaMKII inhibitor, KN-62 (10 μM) on $K_{Ca}3.1$ activator-induced reductions in the phosphorylation of Smad2 proteins in HuT-78 cells. A: Whole protein lysates of DCEBIO (1 μM) and SKA-31 (1 μM)-treated HuT-78 cells in the presence of KN-62 were probed by immunoblotting with anti-Smad2/Smad3 (a, upper panel), anti-phospho-Smad2 (P-Smad2) (b, upper panel), anti-P-Smad3 (c, upper panel), and anti-ACTB antibodies (a-c, lower panels). B, C: Summarized results of the relative expression of P-Smad2/Smad2 and P-Smad3/Smad3 were obtained from the optical density of Smad2/3, P-Smad2, P-Smad3, and ACTB band signals (n=5 for each). Results are expressed as means ± S.D.

Figure 8. Effects of the CaMKII inhibitor, KN-62 (10 μM) on $K_{Ca}3.1$ activator-induced reductions in the nuclear translocation of P-Smad2 in HuT-78 cells. A: Confocal fluorescent images of Alexa Fluor 488-labeled P-Smad2 and P-Smad3 in vehicle-, DCEBIO (1 μM)-, and SKA-31 (1 μM)-treated HuT-78 cells in the presence of KN-62. Nuclear morphologies were shown by DAPI images. Thick and thin dashed lines showed the nuclear boundary and plasma

Molecular Pharmacology Fast Forward. Published on January 8, 2019 as DOI: 10.1124/mol.118.114405
This article has not been copyedited and formatted. The final version may differ from this version.

membrane, respectively. B, C: Summarized results of the expression levels of P-Smad2 (B) and P-Smad3 (C) in the nuclei of HuT-78 cells. The mean fluorescent intensities of nuclear-cytoplasmic ratios were calculated. Results are expressed as means ± S.D. Cell numbers used for the experiments are shown in parentheses.

Molecular Pharmacology Fast Forward. Published on January 8, 2019 as DOI: 10.1124/mol.118.114405
This article has not been copyedited and formatted. The final version may differ from this version.

Fig. 1

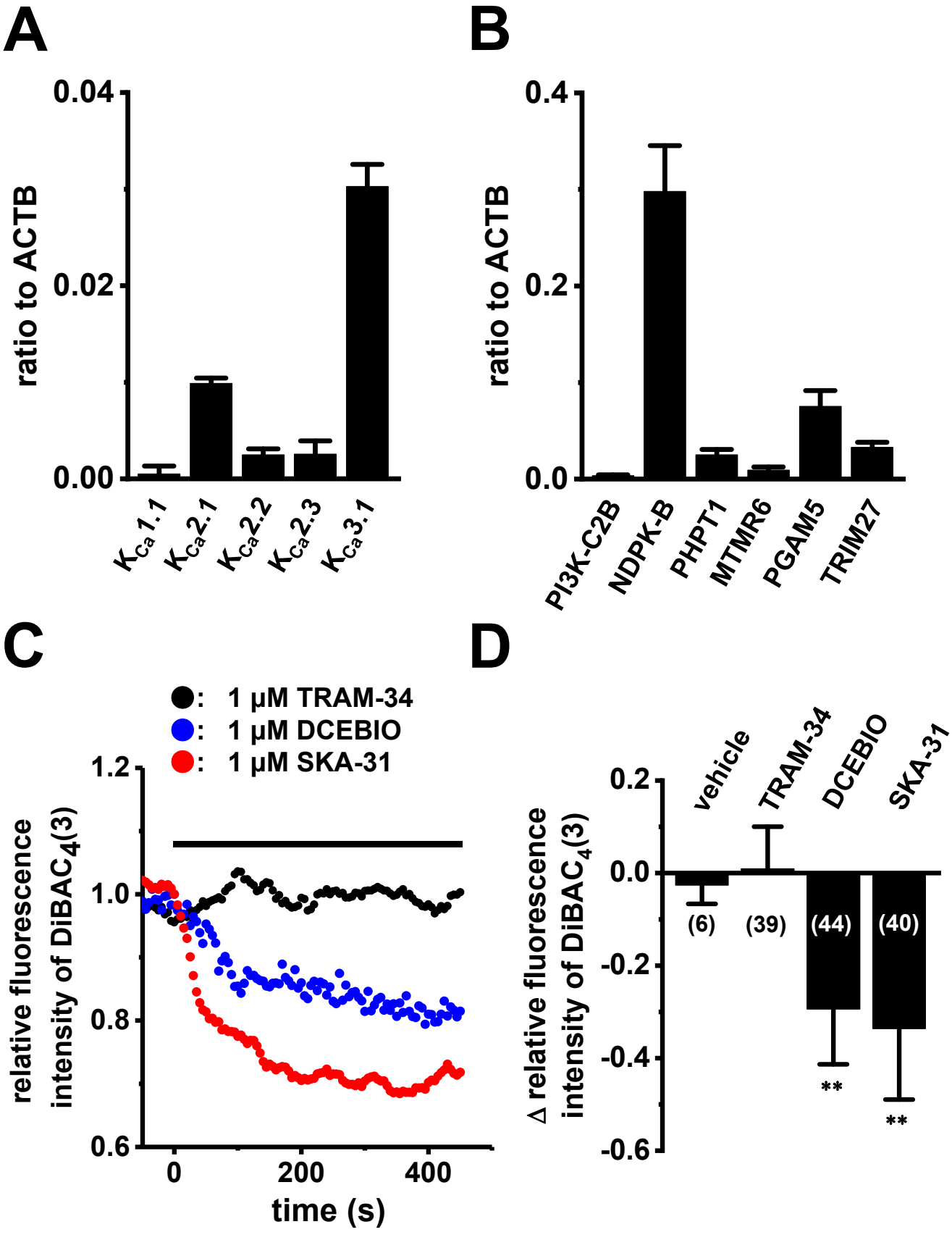

Molecular Pharmacology Fast Forward. Published on January 8, 2019 as DOI: 10.1124/mol.118.114405
This article has not been copyedited and formatted. The final version may differ from this version.

Fig. 1

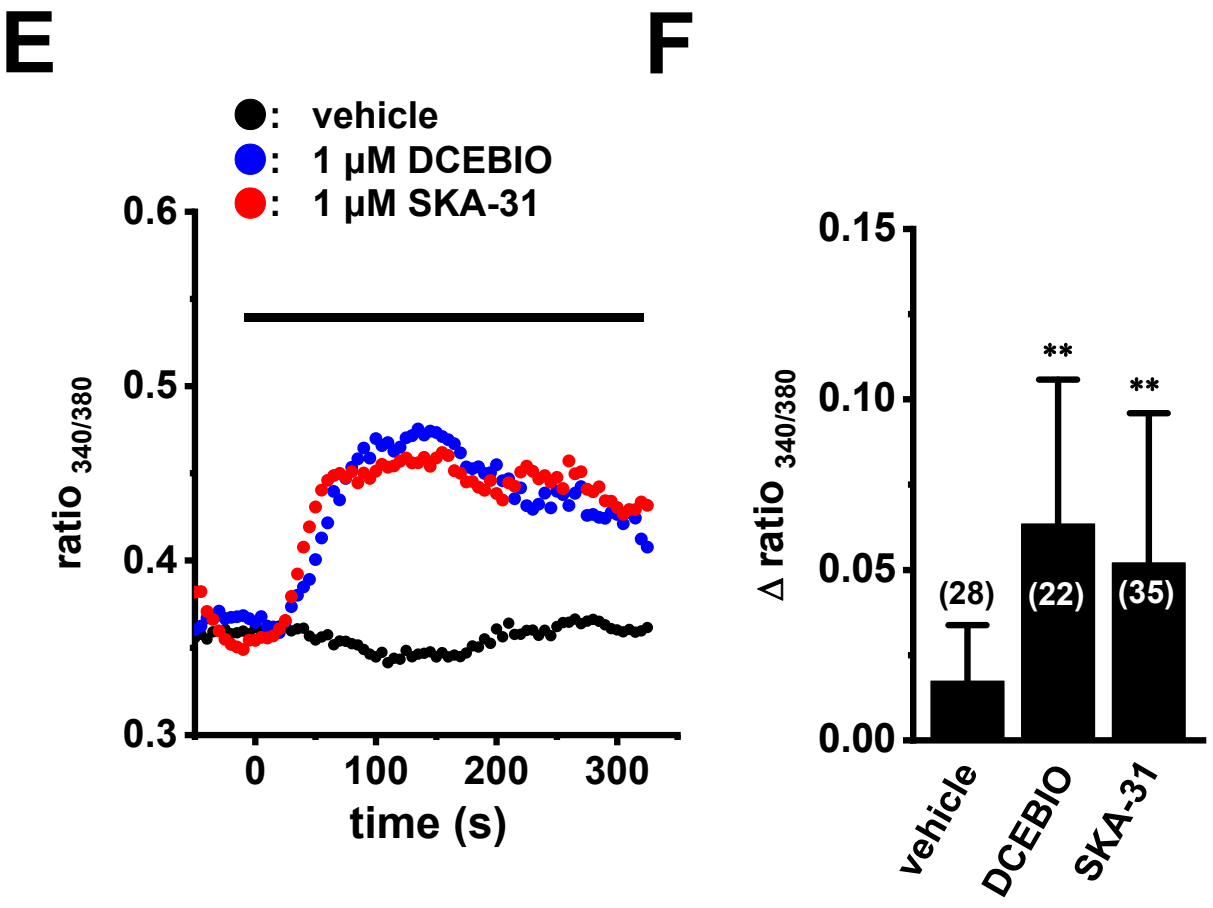

Molecular Pharmacology Fast Forward. Published on January 8, 2019 as DOI: 10.1124/mol.118.114405
This article has not been copyedited and formatted. The final version may differ from this version.

Fig. 2

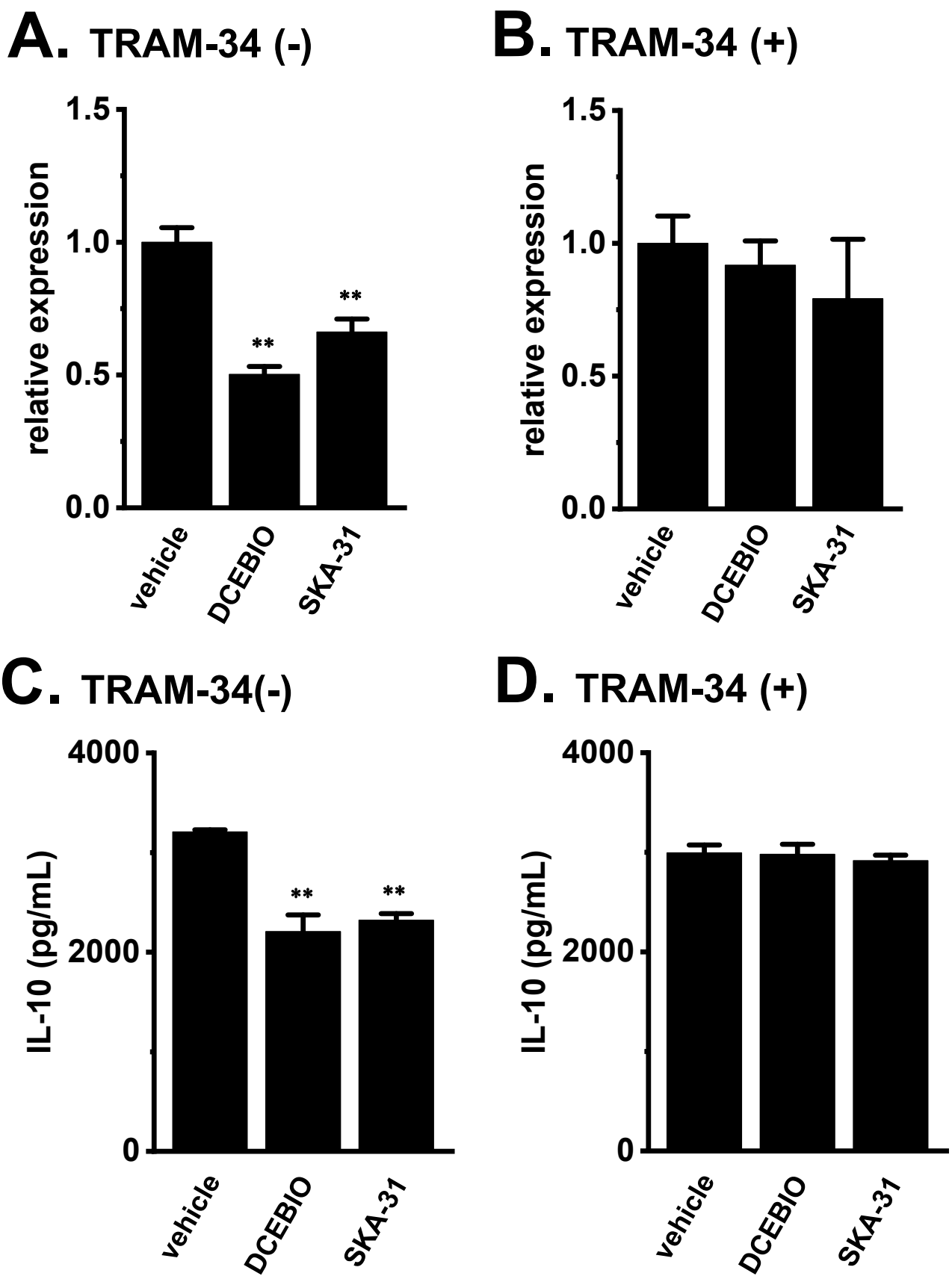

Molecular Pharmacology Fast Forward. Published on January 8, 2019 as DOI: 10.1124/mol.118.114405
This article has not been copyedited and formatted. The final version may differ from this version.

Fig. 3

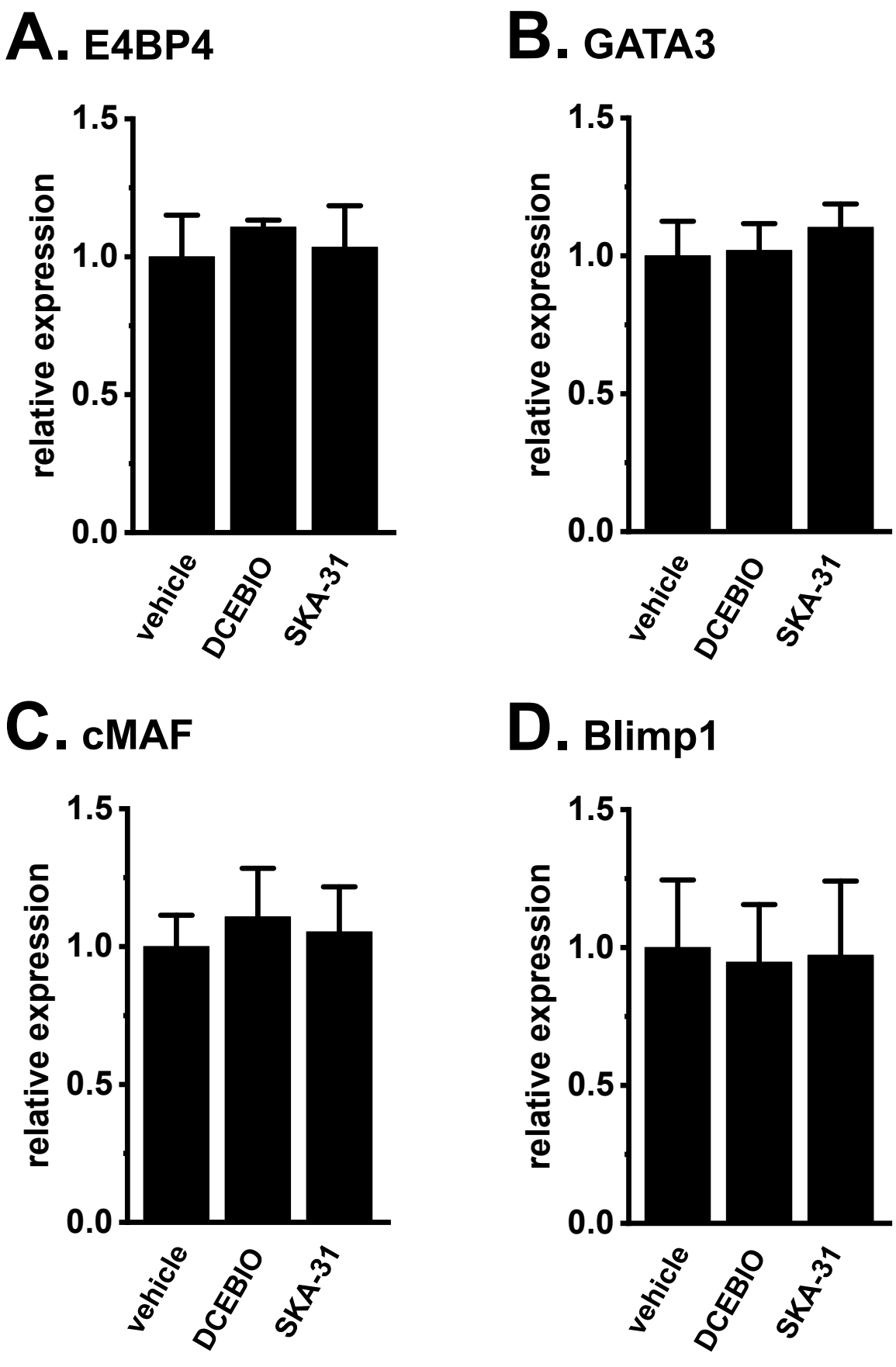

Molecular Pharmacology Fast Forward. Published on January 8, 2019 as DOI: 10.1124/mol.118.114405
This article has not been copyedited and formatted. The final version may differ from this version.

Fig. 4

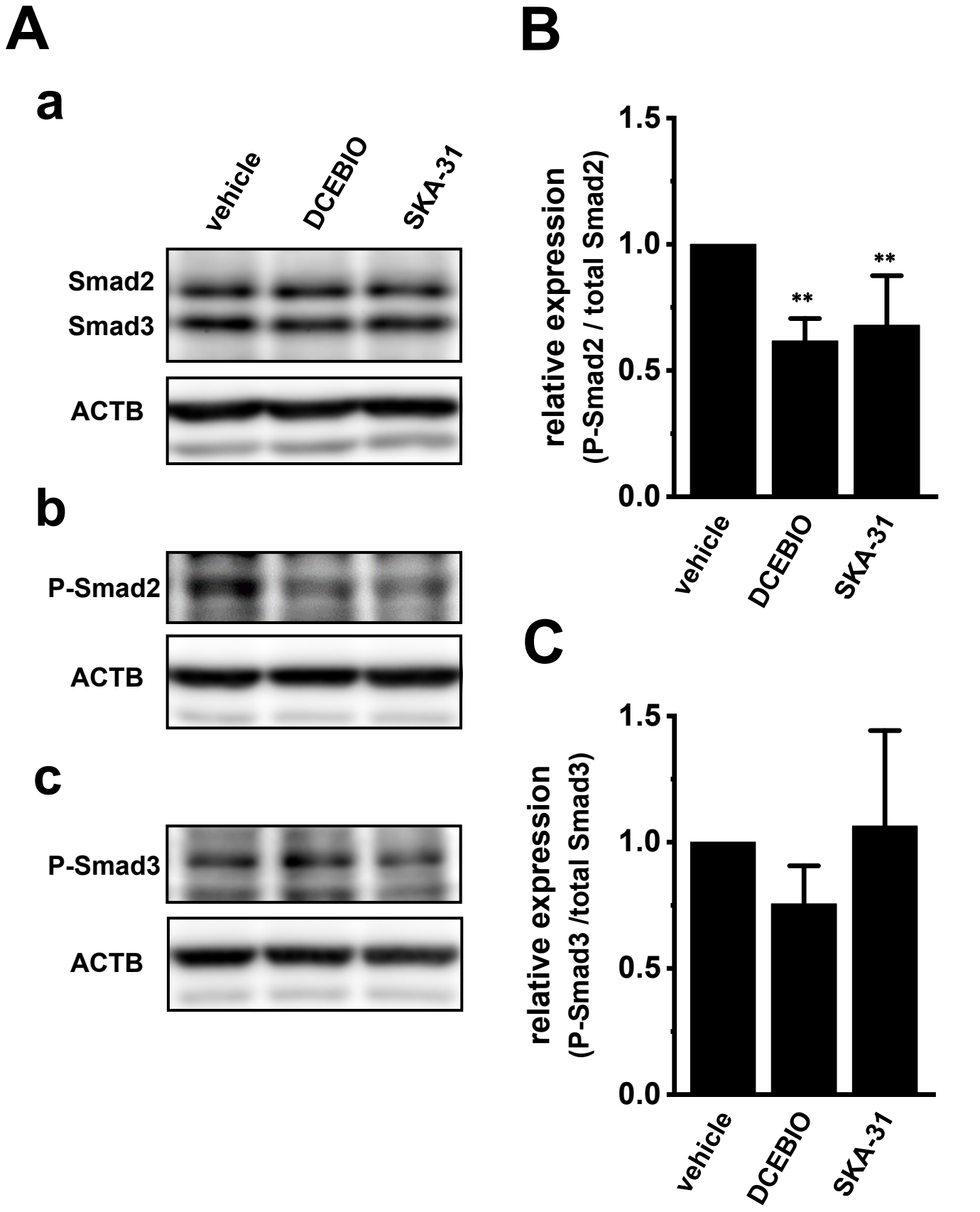

Molecular Pharmacology Fast Forward. Published on January 8, 2019 as DOI: 10.1124/mol.118.114405
This article has not been copyedited and formatted. The final version may differ from this version.

Fig. 5

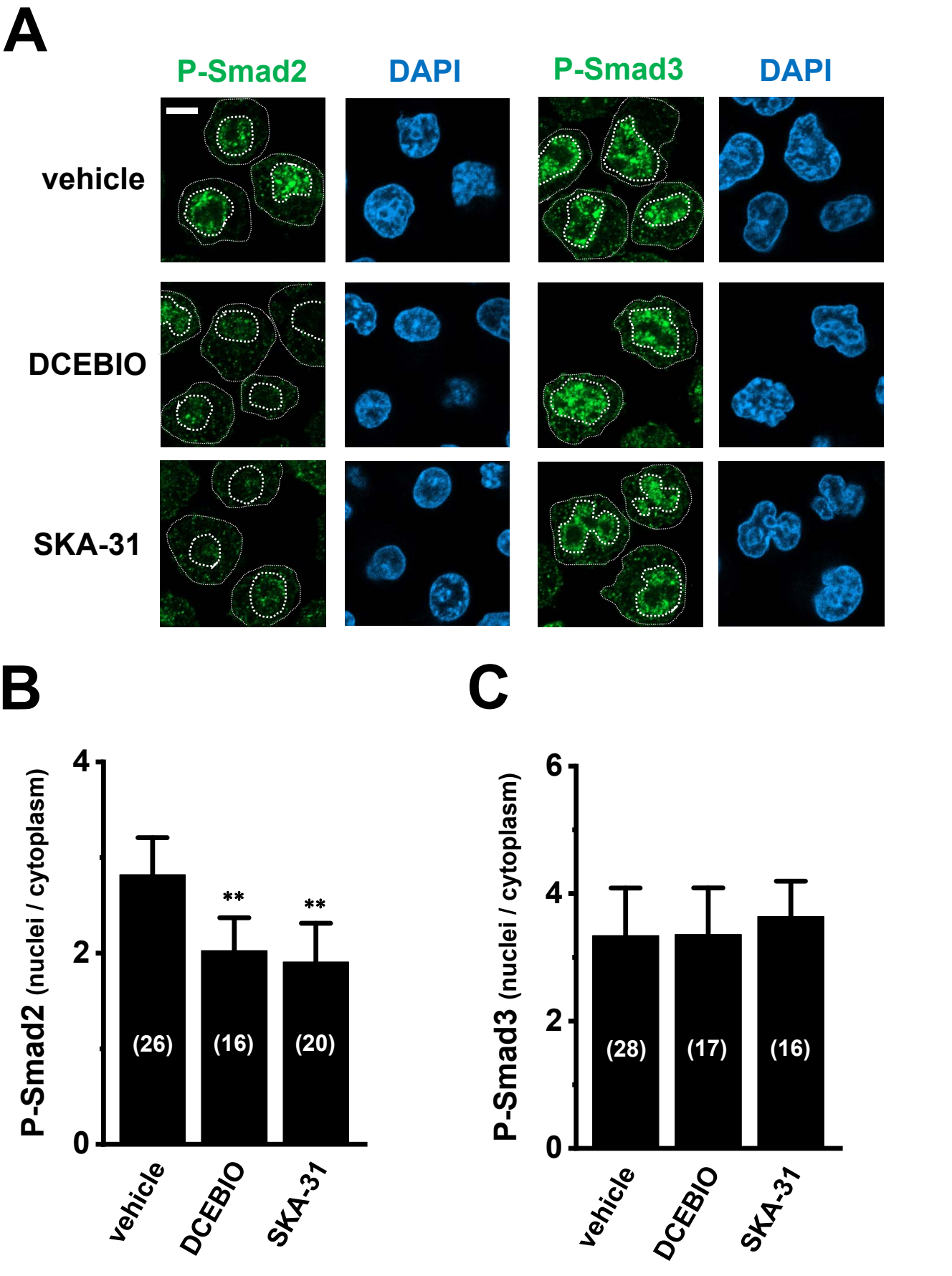

Molecular Pharmacology Fast Forward. Published on January 8, 2019 as DOI: 10.1124/mol.118.114405
This article has not been copyedited and formatted. The final version may differ from this version.

Fig. 6

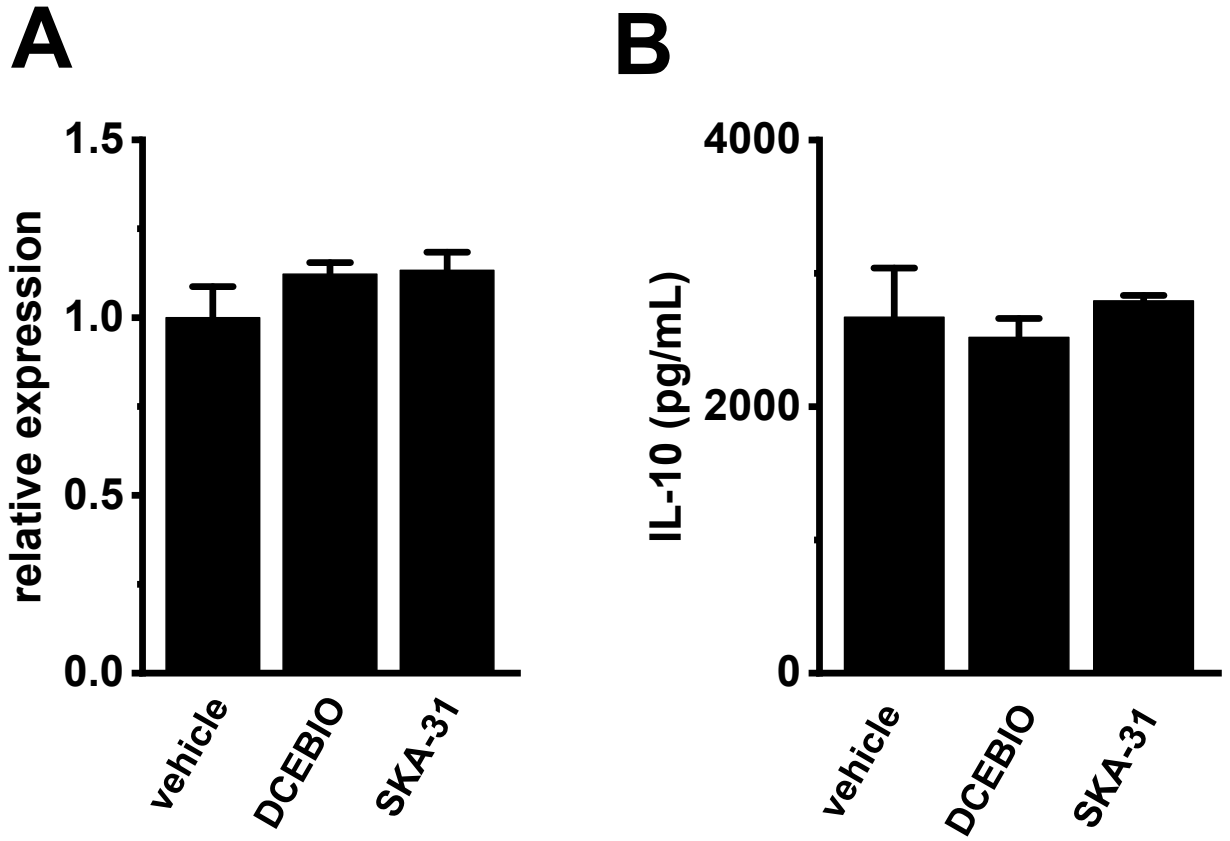

Molecular Pharmacology Fast Forward. Published on January 8, 2019 as DOI: 10.1124/mol.118.114405
This article has not been copyedited and formatted. The final version may differ from this version.

Fig. 7

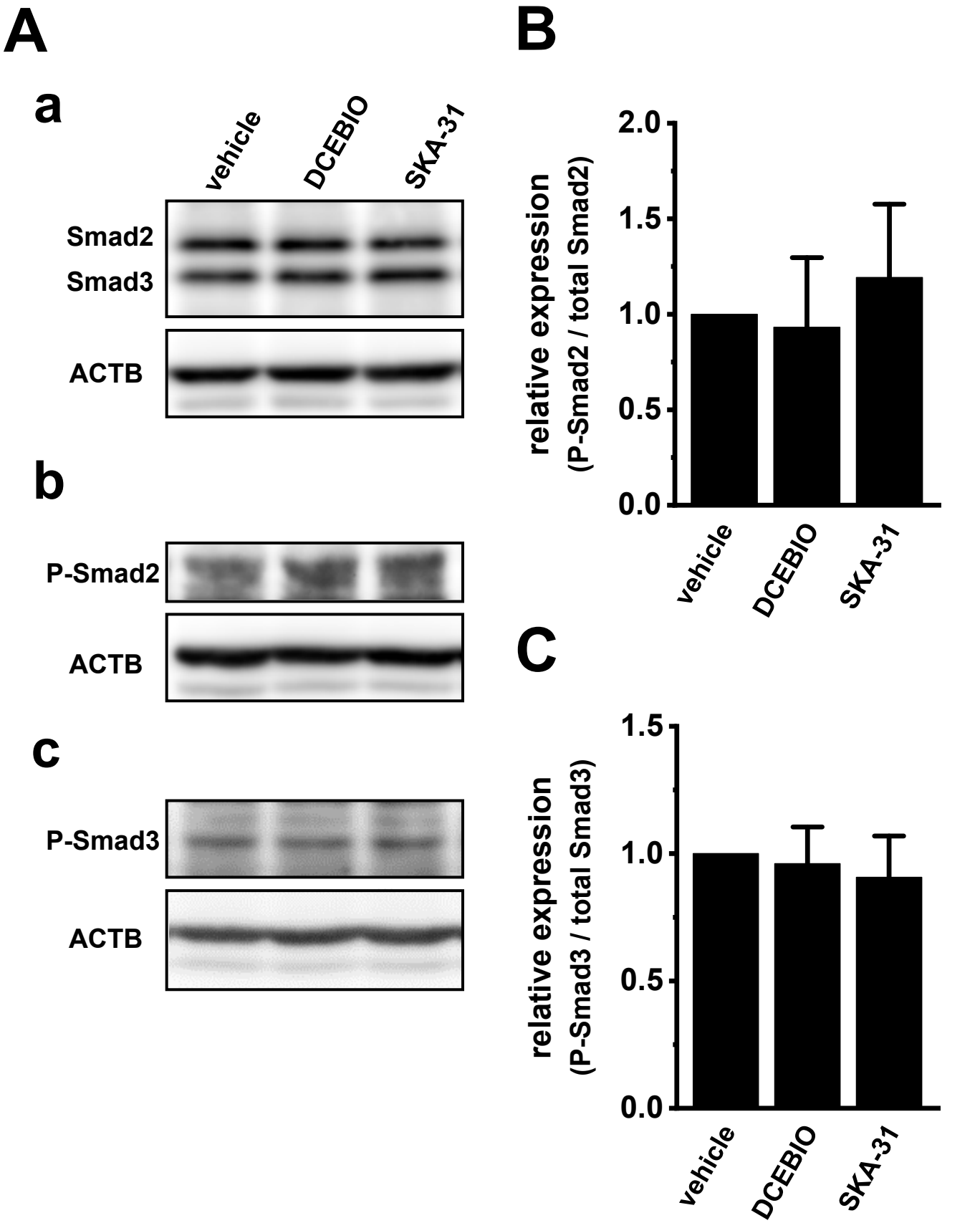

Molecular Pharmacology Fast Forward. Published on January 8, 2019 as DOI: 10.1124/mol.118.114405
This article has not been copyedited and formatted. The final version may differ from this version.

Fig. 8